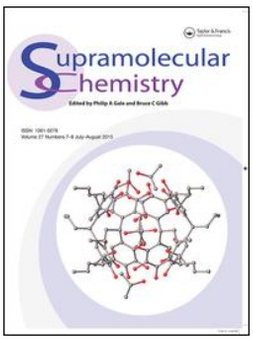

Supramolecular Chemistry

ISSN: 1061-0278 (Print) 1029-0478 (Online) Journal homepage: http://www.tandfonline.com/loi/gsch20

Naphthalene-cholesterol conjugate as simple gelator for selective sensing of CN^- ion

Kumaresh Ghosh & Santanu Panja

To cite this article: Kumaresh Ghosh & Santanu Panja (2016): Naphthalene-cholesterol conjugate as simple gelator for selective sensing of CN^- ion, Supramolecular Chemistry, DOI: 10.1080/10610278.2016.1236926

To link to this article: http://dx.doi.org/10.1080/10610278.2016.1236926

SUPRAMOLECULAR CHEMISTRY, 2016
http://dx.doi.org/10.1080/10610278.2016.1236926

Taylor & Francis
Taylor & Francis Group

Naphthalene-cholesterol conjugate as simple gelator for selective sensing of CN^- ion

Kumaresh Ghosh and Santanu Panja

Department of Chemistry, University of Kalyani, Kalyani, India

ABSTRACT

Cholesterol-based Schiff base **1** has been designed and synthesised. The Schiff base **1** forms yellow coloured gel in DMF:H_2O (2:1, v/v) and the gel is anion responsive. Among different anions, the gel phase of **1** is selectively transformed into sol in the presence of CN^- ions and validates its visual sensing. ^1H NMR, FTIR and HRMS spectroscopic techniques were adopted to study the gelation of **1** and its responsive behaviour towards anions.

ARTICLE HISTORY
Received 20 July 2016
Accepted 11 September 2016

KEYWORDS
Cholesterol; cyanide sensing; supramolecular gelator; anion responsive gel

Cholesterol-based Schiff base **1** has been designed and synthesized. The Schiff base **1** forms yellow colored gel in DMF: H_2O (2:1, v/v) and the gel is anion responsive. Among different anions, the gel phase of **1** is selectively transformed into sol in the presence of CN^- ions and validates its visual sensing.

Introduction

During the past decades, in the field of molecular recognition, building of artificial sensors for anions has brought considerable interest due to the imperative role of anions in environment and biological systems (*1–4*). The competitive nature among basicity, nucleophilicity and hydrogen bonding capability of anions needs precise design of receptor modules that are to provide suitable binding sites for selective recognition of anions (*5–9*). Of the different anions, the sensing of CN^- ion draws attention as it is considered as the most hazardous material for environment due to its slow decomposition rate upon degradation (*10*) and extreme toxicity for living cell (*11*) that may cause death of human beings within several minutes. It can affect adversely the vascular, visual, central nervous, cardiac, endocrine and metabolic systems (*12*).

Till today, synthetic receptors based on hydrogen-bonding principle (*13–18*) as well as metal-anchored simple organic ligand (*19*) are known to act as CN^- detector. Due to interference of other competitive anions, most of them suffer from selectivity. Moreover, nucleophilicity of CN^- enabled to develop reaction-based probes that include addition of CN^- towards cationic boranes, α, β-unsaturated systems, coumarins, hydrazones, amides, aldehydes, ketones, salicyl-imine and so on (*20–22*), where the interference of other anions are efficiently minimised. All these methods involved either fluorometric or colorimetric changes of the receptors in solution. Beside these solution phase studies, the detection of CN^- ion using suitable supramolecular gelators is another approach which is less explored (*23–25*).

Gels are viscoelastic semisolid materials in which the gelator molecules undergo self-association to form three-dimensional matrices. Non-covalent interactions like hydrogen bonding, van der Waals interaction, *π–π* stacking, etc. assist the molecular aggregation of the gelators by

CONTACT Kumaresh Ghosh ghosh_k2003@yahoo.co.in
Supplemental data for this article can be accessed here http://dx.doi.org/10.1080/10610278.2016.1236926.

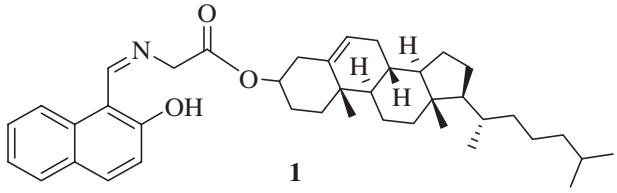

Figure 1. Structure of compound **1**.

immobilising large volume of solvents (*26–28*). During our ongoing research in designing anion responsive supramolecular gelators (*29–33*), herein we wish to report a simple naphthalene–cholesterol coupled Schiff base **1** that forms gel in DMF:H_2O (2:1, v/v) solvent. The gel of **1** exhibits an efficient visual response towards CN^- ion through gel to sol transition which is associated with a colour change from yellow to brown (Figure 1).

Results and discussion

Synthesis

Compound **1** was synthesised according to the Scheme 1. Reaction of cholesterol with chloroacetyl chloride afforded compound **2** which on reflux with NaN_3 in CH_3CN gave the cholesterol azide **3** (*31*). Reduction of the azide **3** using PPh_3/H_2O yielded corresponding amine **4** which on reaction with 2-hydroxy-1-napthaldehyde in dry benzene introduced the compound **1** in appreciable yield.

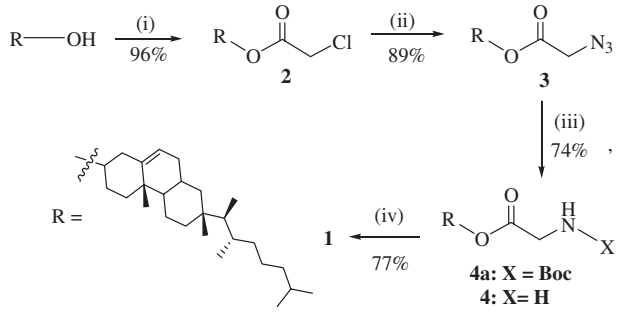

Scheme 1. (i) Chloroacetyl chloride, pyridine, dry CH_2Cl_2, rt, 10 h; (ii) CH_3CN, NaN_3, Reflux, 5 h; (iii) (a) PPh_3, THF, H_2O, rt, 4 h; (b) $(BOC)_2O$, Et_3 N, dry THF, rt, 6 h; (c) TFA, dry CH_2Cl_2, rt,1 h; (iv) 2-hydroxy-1-napthaldehyde, dry benzene, reflux 12 h.

Gelation study

Structure **1** is the fascinating integration between naphthalene chromophore and the cholesterol phase via imine bond formation and these different segments play crucial role during gelation. The naphthylaldimine group locks the molecular conformation in planar arrangement by forming intramolecular hydrogen bond that results in extensive π–π stacking between the naphthalene rings (*34–36*). The cholesteryl part with large hydrophobic surface triggers the intermolecular association through van der Waals interaction (*37, 38*). The gelation ability of **1** was examined in a wide range of solvents with different polarities (Table 1S). While in non-polar solvents compound **1** remained either soluble or partially soluble, it formed yellow coloured gel in DMF:H_2O (2:1, v/v) at a minimum concentration of 12 mg/mL.

Morphology, rheology studies and thermal stability of gels

The gel was stable at room temperature and exhibited thermally activated gel–sol reversible transition (Figure 1S). The gel melting temperature at mgc was recorded to be 62 °C and a sharp increase in T_{gel} was observed with higher gelator concentration (Figure 2S). The morphology of the gel was characterised by SEM images that revealed closely spaced plate like matrix (Figure 2(A)). The rheology experiment (Figure 2(B)) was carried out to examine the mechanical properties of the gel. Variation of stress amplitudes and frequencies for the gel exposed that the dynamic storage modulus G′ was always greater than the corresponding loss modulus G″ over the range studied. The stress sweep experiment at a fixed frequency (ω = 10 rad/s) gave a non-linear response of both G′ and G″ but no prominent crossover point was found within the experimental stress region. In frequency sweep experiment at a constant strain of 1%, both G′ and G″ were found to be frequency independent and exhibited more than five order higher magnitude of G′ than those of G″ at any frequency. These results corroborated the viscoelastic nature of the gel.

To our opinion, the gel formation of **1** may be attributed to the aggregation of the gelators according to the probable mode shown in Figure 3(A). In this regard, FTIR spectra of **1** in its amorphous and gel states (Figure 3S) were recorded to get some idea about the mechanism of gelation. In both amorphous and gel states, the stretching for –C=N appeared at 1636 cm^{-1} remained unaffected. This suggested the existance of strong intramolecular H-bond with the –OH group. In addition, the stretching frequency for ester carbonyl of **1** appeared at 1750–1743 cm^{-1} in amorphous state moved to 1755–1742 cm^{-1} in gel state. This small shift is presumably due to involvement of ester carbonyl in hydrogen bonding with water of the medium probably via water linking during gel formation. We also believe that π–π stacking between the naphthalene rings and the hydrophobic–hydrophobic interaction between the cholesterol units stabilize the network. A shouldering in the region 310–350 nm in UV–vis spectrum of **1** in gel state with respect to its sol state and 4 nm red shift of the absorption at 400 nm in solution corroborates

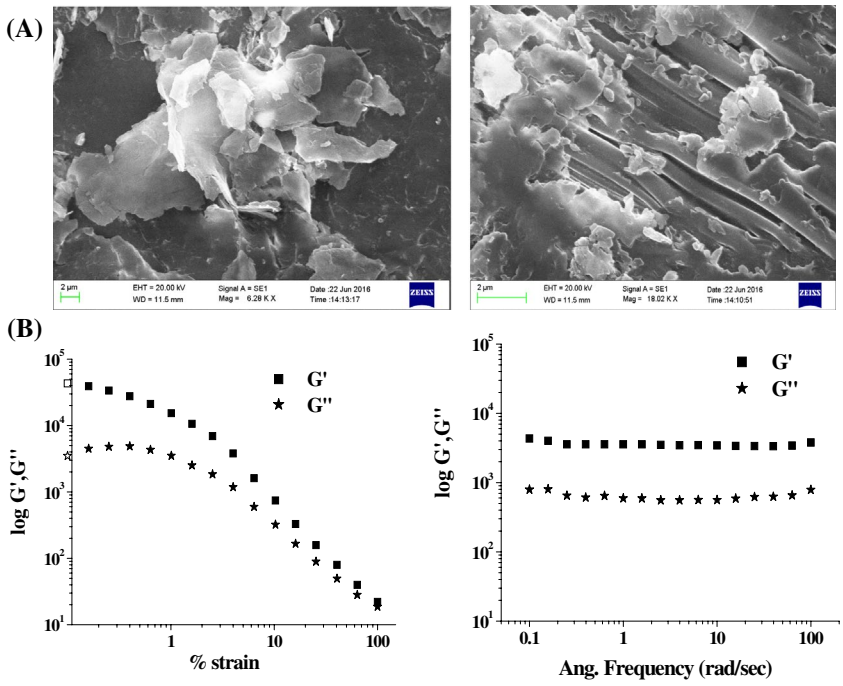

Figure 2. (A) SEM images of xerogel of **1** and (B) Rheology experiment of gel **1** in DMF:H2O (2:1, v/v).

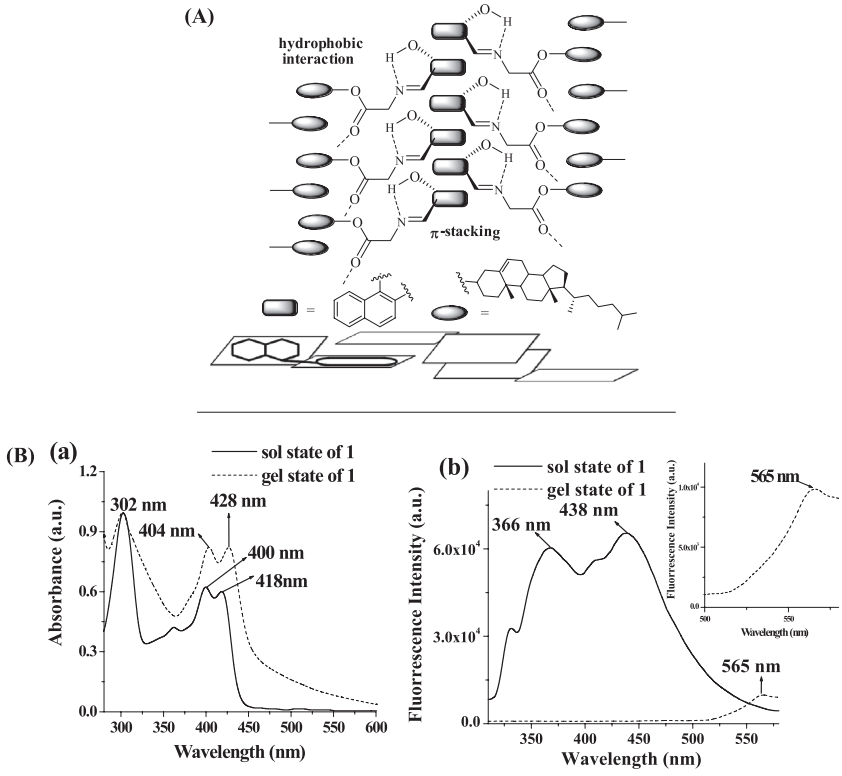

Figure 3. (A) Suggested modes of interaction of **1** in gel state; (B) Comparison of (a) normalised UV–vis and (b) fluorescence spectra (λ_{ex} = 300 nm) of **1** in the sol and gel states [solution of **1** was prepared in CH_3CN containing 1% $CHCl_3$].

the aggregation (Figure 3(B-a)). Moreover, a red shift of 10 nm in the absorption band at 418 nm during gelation is a clear indication of *π–π* stacking (J aggregates) between the naphthalene rings (*39–41*). This is in accordance with the observation of Niu et al. in other related systems (*36*). Furthermore, in fluorescence, the quenching of emissions centred at 366 and 438 nm in solution (CH_3CN containing 1% $CHCl_3$) with the appearance of new band at 565 nm

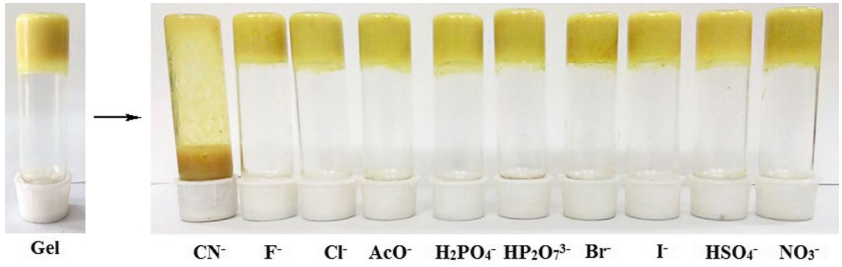

Figure 4. Photograph showing the phase changes of **1** (15 mg/mL) in DMF:H_2O (2:1, v/v) in presence of 5 equiv. amounts of different anions [c = 1 M in H_2O as perchlorate salt] after 8 h.

in the gel state (Figure 3(B-b)) explains the overlapping of naphthalene rings to form higher order of π–π stacking aggregation in gel matrix (*42, 43*). The quenching of emission in such case is known as 'aggregation-caused quenching' (*44*). In this context, the study of concentration-dependant fluorescence of **1** in solution is worth mentioning (Figure 4S). As the concentration of **1** is increased, the monomer emission of naphthalene was reduced with the appearance of red-shifted emission at 468 nm for stacked naphthalenes. The emissions for stacked naphthalenes at 565 and 468 nm in the gel and sol states, respectively, are presumably attributed to the difference in energy of the excited states of naphthalene in two different states for which the energy gap for transitions varies.

Anion responsive behaviour in both gel and sol states

The stimuli responsive nature of the gel was investigated by adding concentrated solutions of different anions (counter cations: tetrabutylammonium ions) on the top of the gel at room temperature (Figure 4). Among the different anions studied, the gel state of **1** was converted into solution only in presence of 5 equiv. amounts of CN^- ions after 8 h with a colour change from yellow to brown. Under similar conditions, the gel phase remained unaffected in presence of other anions such as F^-, Cl^-, Br^-, I^-, AcO^-, $H_2PO_4^-$, $HP_2O_7^{3-}$, HSO_4^- or NO_3^- ions (Figure 4). To understand the sensitivity of the gel towards CN^- ions, different amounts of CN^- ions were added to the gel (Figure 5S). In presence of 1 equiv. amount of CN^-, disruption of the gel into the sol took longer time. These results suggest that the gelator **1** is highly selective in visual detection of CN^- ion.

The gel to sol transition of **1** in the presence of CN^- may be due to either deprotonation of phenolic –OH or nucleophilic addition of CN^- ion to the activated –C=N or ester carbonyl group. To establish this fact, ^1H NMR and FTIR of **1** were recorded before and after addition of CN^- ions. In ^1H NMR, recorded in $CDCl_3$ solvent, the disappearance of the signal at 14.68 ppm for –OH (hydrogen bonded) of **1** in the presence of equiv. amount of TBACN (tetrabutylammonium cyanide) supported the deprotonation phenomena (Figure 5(A)) (*45, 46*). On deprotonation, the aromatic protons displayed small upfield chemical shift. The imine proton (H_b) underwent 0.11 ppm upfield chemical shift which clearly explained the persistence of the imine bond in the interaction process. Deprotonation of H_a was also observed in the presence of F^- (Figure 6S) (0.10 ppm upfield shift of the proton H_b). In contrast, in the presence of CN^-, the signal for H_c proton moved upfield by 2.07 ppm. During the event, proton of type 'd' which appeared at 4.74 ppm as multiplet also underwent small upfield shift (0.15 ppm). Such change in positions of the signals for the indicated protons recommended the formation of CN^- adduct on nucleophilic attack to ester carbonyl of **1**. FTIR study also revealed the disappearance of the signal at 1743 cm^{-1} for the ester carbonyl stretching upon interaction with CN^- ion in solution phase (Figure 7S).

The CN^--adduct formation was also confirmed by mass spectral analysis (Figure 5(B)). In HRMS spectrum, a major peak at m/z 663.4462 that corresponds to $(M + CH_3CN\text{-}1)^+$ [calcd. 663.4218] was observed upon treatment of **1** with CN^-.

Cyanide-induced gel to sol conversion of **1** due to nucleophilic attack of CN^- onto the ester carbonyl was also realised by FTIR study. In this case, the ester carbonyl stretching at 1742 cm^{-1} was abolished with the appearance of a new stretching at 2169 cm^{-1} for cyanide motif (Figure 7S). In the event, negligible change in –C=N stretching corroborated the persistence of the imine bond in the presence of CN^- ion.

In order to understand the solution phase interactions, we performed UV–vis and fluorescence titrations of **1** ($c = 2.50 \times 10^{-5}$ M) with the said anions (counter cations:tetrabutylammonium ions; $c = 1.0 \times 10^{-3}$ M) in CH_3CN containing 1% $CHCl_3$. In UV–vis, compound **1** initially exhibits three absorbtion maxima at 302 nm, 404 nm and 418 nm. During titration, the intensity of these three peaks was decreased by almost equal extent for all anions except CN^- (Figure 8S). A weak ratiometric response with an isosbestic point at 430 nm was observed on gradual addition of CN^- ions (Figure 6(a)). In fluorescence, compound **1** did

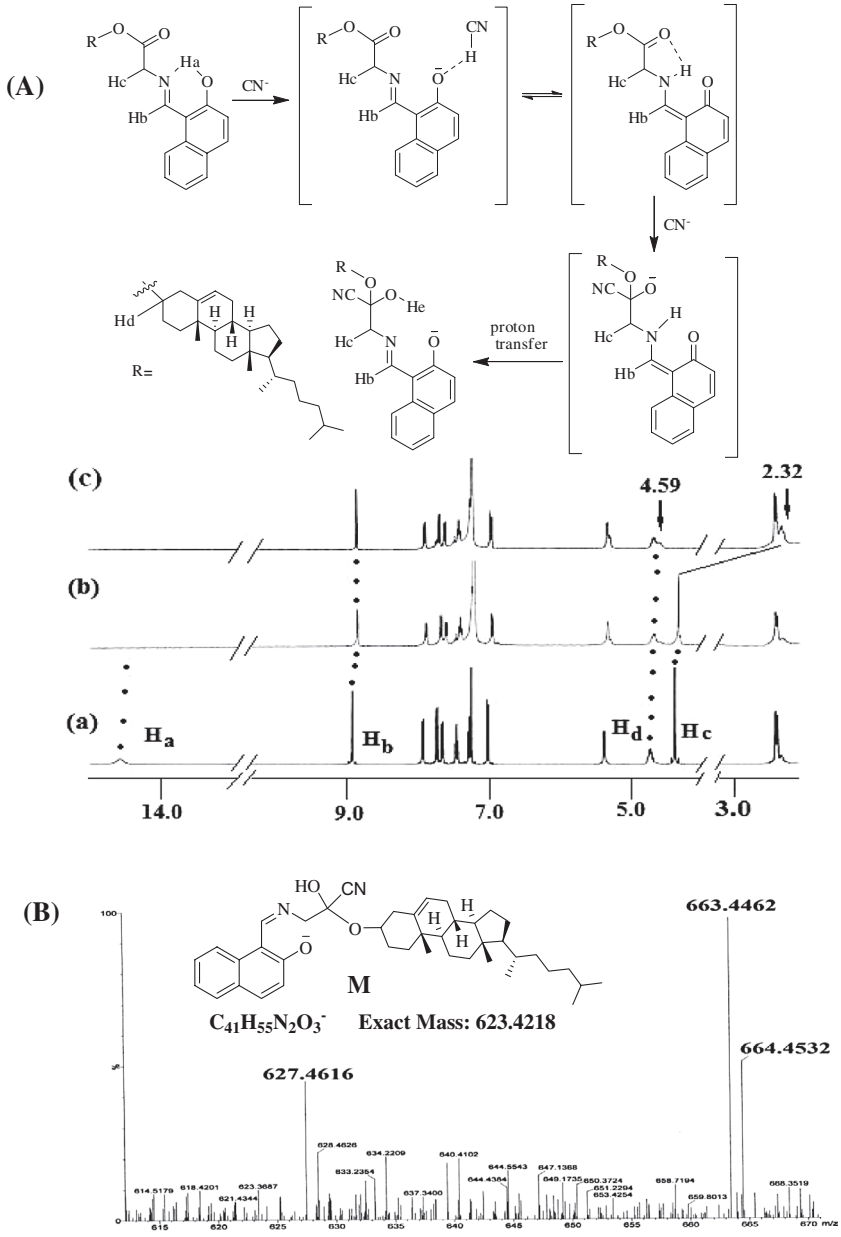

Figure 5. (A) Partial ^{1}H NMR (400 MHz) spectral of (a) **1** [$c = 1.18 \times 10^{-2}$ M], (b) **1** with equiv. amount of TBACN and (c) **1** with 2 equiv. amount of TBACN in $CDCl_3$ with a probable mechanism; (B) HRMS spectra for the cyanide adduct of **1**.

not show any selectivity towards anions (Figure 9S). Upon excitation at 300 nm, compound **1** exhibited two emission peaks at 366 nm and 438 nm for monomer and excimer emissions, respectively. The monomer emission is attributed to the excited state proton transfer (*47, 48*) from the phenol hydrogen to the imine nitrogen atom. In presence of the basic anions like CN^-, F^- and $HP_2O_7^{3-}$, deprotonation of phenolic –OH resulted in formation of weakly basic phenoxide ion that tuned the excited state charge transfer (*47, 48*) (ESCT) process from the phenoxide ion to the imine bond. Facilitation of ESCT resulted in generation of a new peak at 460 nm in the emission spectra of **1** in the presence of above said anions. Upon gradual addition of CN^- (Figure 6(b)), F^- and $HP_2O_7^{3-}$ (Figure 10S) the intensity of the emission at 460 nm underwent significant enhancement that resulted in an overall red shift of 22 nm from the initial emission maxima of 438 nm. Other anions taken in this study had negligible effect on emission of **1** (Figure 10S). The Benesi–Hildebrand plot (*49*) of the change in emission intensity of **1** against the reciprocal of anion concentration gave a linear fit, characteristic of 1:1 complexation from which the association constant was estimated to be 1.56×10^2 M^{-1}, 1.59×10^2 M^{-1} and 1.81×10^2 M^{-1} for CN^-, F^- and $HP_2O_7^{3-}$, respectively (Figure 11S). The detection limit (*50*) for CN^- was determined to be 1.35×10^{-5} M (Figure 12S). However, addition of Ca^{2+} ions ($c = 5.0 \times 10^{-3}$ M) to the ensemble of

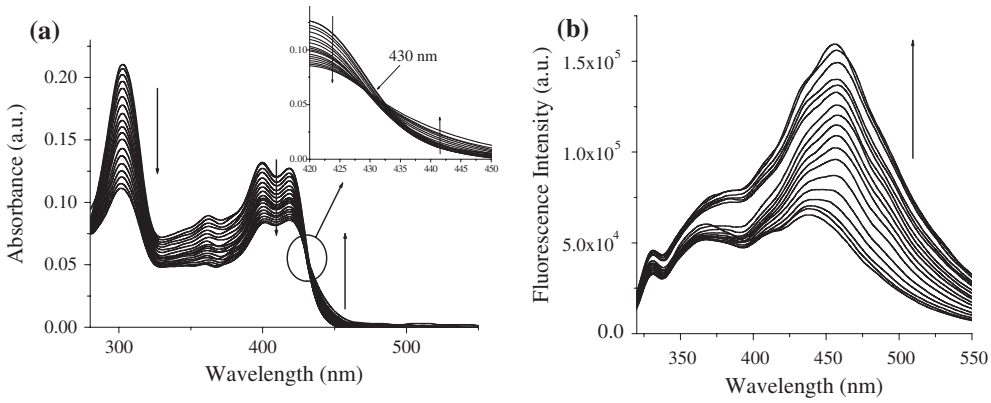

Figure 6. Change in absorbance (a) and emission (b) spectra of **1** ($c = 2.50 \times 10^{-5}$ M) upon addition of TBACN ($c = 1.0 \times 10^{-3}$ M) in CH_3CN containing 1% $CHCl_3$.

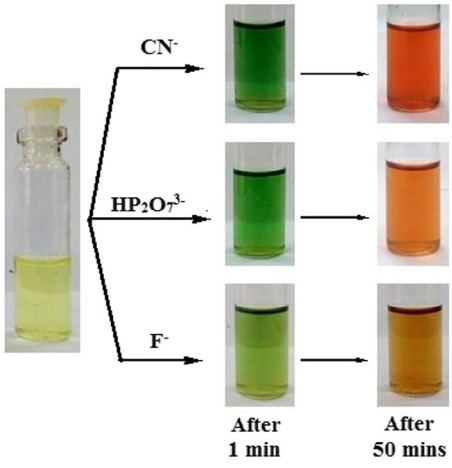

Figure 7. Pictorial representation of the colour changes of **1** ($c = 1.0 \times 10^{-3}$ M) in the presence of equiv. amount of respective anions ($c = 5.0 \times 10^{-3}$ M) with time in CH_3CN containing 4% $CHCl_3$.

1 with F^- resulted in almost recovery of the initial emission bands probably due to scavenging of F^- ions through the formation of CaF_2 (Figure 13S). Under similar conditions, individual ensembles of **1** with CN^- and $HP_2O_7^{3-}$ exhibited negligible changes in emission spectra upon addition of Ca^{2+} ions. Only 12 nm and 15 nm blue shifts were observed for CN^- and $HP_2O_7^{3-}$ ensembles, respectively. These studies clearly revealed that the basicity and the hydrogen bonding ability of the anions seemed to play major role for the changes in the emission spectra of **1**, and therefore resulted less selectivity for cyanide in solution.

These observations create contradiction with the gel phase interactions of **1** with anions that resulted in selective phase transition in the presence of CN^-. This occurs due to different solvent systems considered in gel and solution phase interactions. To be confirmed, the solution phase interaction of **1** with the said anions in DMF/H_2O (2:1 v/v) was carried out. In this case, the change in absorbance and fluorescence was marked and selective only to CN^- ion when it was added in higher equiv. amounts to the solution of **1** (Figures 14S and 15S) and showed consistency with the gel phase observations.

However, in order to correlate the bulk phase interactions of **1** with the solution phase in CH_3CN, time-dependent UV–vis and fluorescence spectra of **1** in the presence of CN^- ions at high concentration were recorded in CH_3CN containing 4% $CHCl_3$ ($CHCl_3$ was used for homogeneity). In this case, a ratiometric nature in the absorption spectra of **1** ($c = 1.0 \times 10^{-3}$ M) was observed with time in the presence of equiv. amount of CN^- ($c = 5.0 \times 10^{-3}$ M) ions. Initially, a charge transfer band at 658 nm (within 1 min) in the absorption spectra due to generation of naphthoxide ion was noted and the colour of the solution changes from yellow to deep green (Figure 7). With time the intensity of this peak was decreased with simultaneous generation of a new band at 490 nm (Figure 8(a)) and the colour of the solution was changed into rose red. In case of $HP_2O_7^{3-}$, similar spectral behaviour with colour change of the solution was observed as that of CN^- ions but in lesser extent whereas F^- ions did not bring about any noticeable change in absorption spectrum of **1** (Figure 16S). Figure 8(b), in this regard, represents time-dependent change in absorbance of **1** in the presence of equiv. amount of above-mentioned anions. In fluorescence, compound **1** initially exhibited almost similar behaviour in emission spectra in the presence of said three anions (Figure 17S). On progression, while the ensemble of **1** with CN^- showed fluorescence quenching (Figure 8(c)), the other ensembles exhibited turn on in emission at 468 nm with time (Figure 18S). A plot of change in emission intensities against time (Figure 8(d)) clearly revealed that initially, due to accumulation of large amounts of basic anions, rapid formation of naphthoxide ions favoured ESCT process which on progression is repressed by the keto-enol equilibrium in solution. Close proximity of –NH of keto form (Figure 5(A)) trigger the

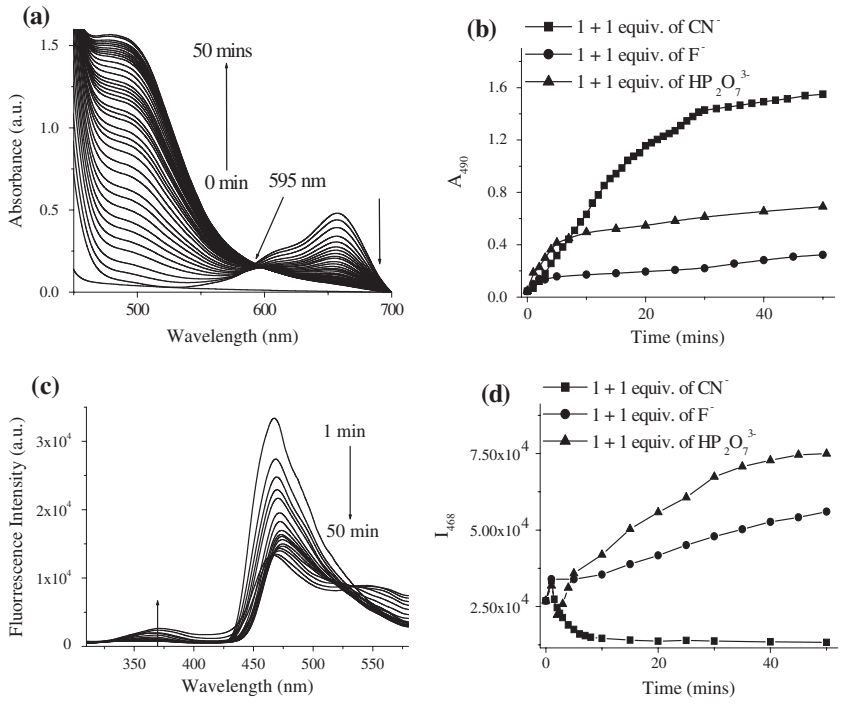

Figure 8. (a) Time-dependent UV–vis spectra of **1** containing equiv. amount of CN^-; (b) change in absorbance of **1** with time containing equiv. amount of different anions; (c) time-dependent emission spectra of **1** containing equiv. amount of CN^-; (d) change in emission intensities of **1** with time containing equiv. amount of different anions; [conc. of **1** = 1.0×10^{-3} M, conc. of anions = 5.0×10^{-3} M in CH_3CN containing 4% $CHCl_3$].

CN^- addition to ester carbonyl of **1** and validates the cyanide adduct formation as described in Figure 5.

Conclusion

In conclusion, naphthalene–cholesterol conjugate **1** has been designed and synthesised. Hydrogen bonding effect of the salicylaldimine like group in **1** resulted in extensive *π–π* stacking between the naphthalene rings which assists gel formation through extended intermolecular aggregation of **1** in DMF:H_2O (2:1, v/v) mixture solvent. The aggregation is further stabilized by large hydrophobic surface provided by cholesterol moiety in **1**. The gel as obtained in DMF:H_2O (2:1, v/v) is found to be thermo reversible and anion responsive. CN^- ion over a series of other anions causes rapid gel to sol transition with a colour change from yellow to brown and validates its visual sensing. ^1H NMR, FTIR and HRMS spectroscopic techniques unequivocally suggested the formation of CN^- adduct via the nucleophilic addition to the ester carbonyl of **1**. Fluorescence study of **1** in CH_3CN containing 1% $CHCl_3$ interprets the detection of CN^- ions by showing turn-on emission but suffers from less selectivity due to interference of other basic anions like F^- and $HP_2O_7^{3-}$. However, increase in concentration of **1** in solution brought about selectivity towards CN^- ion with a distinguished colour change of the solution from yellow to rose red. Thus, the simple design-based molecule **1** has been established as a good candidate for selective naked eye detection of CN^- ion in both gel and sol states. Further insight along this direction is underway in our laboratory.

Experimental

Materials

Cholesterol was purchased from Spectrochem. Pyridine, chloroacetyl chloride, sodium azide, PPh_3, $(Boc)_2O$, Et_3N, were obtained from Spectrochem. Tetrabutylammonium salts of anions used in the study were purchased from Sigma-Aldrich and were carefully handled. All solvents used in the synthesis were purified, dried and distilled as required. Solvents used in NMR experiments were obtained from Aldrich. Thin layer chromatography was performed on Merck precoated silica gel 60-F_{254} plates. ^1H and ^{13}C NMR spectra were recorded using Bruker 400 MHz instrument using TMS as internal standard. High resolution mass data were acquired by the electron spray ionisation technique on XEVO GS-2 QTOf Waters mass spectrometer. FTIR measurements of all the compounds and dried gels (xerogels) were carried out using a Perkin-Elmer L120-00A spectrometer (ν_{max} in cm^{-1}) using KBr cell and KBr pellets, respectively. Scanning electron microscopy (SEM) images were obtained on EVO LS-10 ZEISS instrument. Fluorescence and UV–vis studies were performed using

Horiba Fluoromax 4C spectrofluorimeter and Shimadzu UV-2450 spectrophotometer, respectively.

Syntheses

Chloro-acetic acid 17-(1,5-dimethyl-hexyl)-10,13-dimethyl-2,3,4,7,8,9,10,11,12,13,14,15,16,17-tetradecahydro-1H-cyclopenta[a]phenanthren-3-yl ester (2)

To a stirred solution of cholesterol (0.5 g, 1.29 mmol) in 20 mL dry CH_2Cl_2 was added chloroacetyl chloride (0.16 mL, 1.93 mmol) and pyridine (0.05 mL, 0.65 mmol) under nitrogenous atmosphere. The mixture was allowed to stir for 10 h at room temperature. After completion of reaction, the solvent was evaporated and the crude was extracted with $CHCl_3$ (3 × 30 mL). The organic layer was washed several times with water and separated and dried over Na_2SO_4. Evaporation of the solvent gave white solid compound. Recrystallisation from petroleum ether afforded pure product **2** (0.58 g, yield 96%), mp 148 °C. ^{1}H NMR (400 MHz, $CDCl_3$) δ 5.37 (m, 1H), 4.72 (m, 1H), 4.03 (s, 2H), 2.36 (m, 2H), 2.02–0.85 (m, 38H), 0.67 (s, 3H); FTIR (KBr, cm^{-1}): 2939, 2907, 2821, 1753, 1620, 1195.

Azido-acetic acid 17-(1,5-dimethyl-hexyl)-10,13-dimethyl-2,3,4,7,8,9,10,11,12,13,14,15,16,17-tetradecahydro-1H-cyclopenta[a]phenanthren-3-yl ester (3)

To a stirred solution of compound **2** (0.5 g, 1.08 mmol) in CH_3CN (20 mL) NaN_3 was added (0.11 g, 1.6 mmol) and the reaction mixture was refluxed for 5 h. The progress of reaction was monitored by TLC. After the total consumption of the halide, solvent was evaporated off and water was added. The reaction mixture was extracted with $CHCl_3$. Evaporation of the solvent gave the crude azide product **3** (0.45 g, yield 89%, mp 116 °C), which after recrystallisation from diethyl ether was directly used in the next step. FTIR (KBr, cm^{-1}): 2938, 2107, 1747, 1213.

(8R,9R,10S,13S,14R,17S)-10,13-dimethyl-17-((S)-6-methylheptan-2-yl)-2,3,4,7,8,9,10,11,12,13,14,15,16,17-tetradecahydro-1H-cyclopenta[a]phenanthren-3-yl 2-aminoacetate (4)

Compound **4** was obtained from compound **3** via a three step reaction. Initially, to a stirred solution of compound **3** (1 g, 2.12 mmol) in 25 ml THF containing four drops of water, PPh_3 (1.66 g, 6.36 mmol) was added and the reaction mixture was allowed to stir at room temperature for 4 h. A solution of $(Boc)_2O$ (0.92 g, 4.24 mmol) in 10 mL of THF was added to the reaction mixture followed by the addition of 0.62 mL of Et_3N (4.24 mmol). The reaction mixture was stirred at the room temperature for 6 h. Then the solvent was removed under vacuum and the crude mass was extracted with $CHCl_3$. The Boc- protected crude mass was purified by column chromatography using 40% ethyl acetate – petroleum ether as eluent to afford compound **4a** in 96% yield (1.1 g). ^{1}H NMR ($CDCl_3$, 400 MHz): δ 5.38 (d, 2H, *J* = 4 Hz), 5.01 (br t, 1H), 4.68 (m, 1H), 3.88 (d, 2H, *J* = 4 Hz), 2.33 (d, 2H, *J* = 8 Hz), 2.02–0.67 (m, 50H, cholesteryl and methyl protons of Boc-group); FTIR (KBr, cm^{-1}): 3382, 2937, 1753, 1725, 1677.

In the next step, 1.0 g of the Boc- protected compound **4a** (1.83 mmol) was dissolved in 10 mL of dry CH_2Cl_2 and TFA (4.17 g, 36.6 mmol) in 10 ml of dry CH_2Cl_2 was added dropwise at 0 °C. The reaction mixture was stirred at room temperature for 1 h. Then solvent was evaporated under reduced pressure and the crude mass was extracted with $CHCl_3$. The organic layer was washed with aq. $NaHCO_3$ solution (15 mL × 3) and dried over anhydrous Na_2SO_4. The solvent was concentrated under reduced pressure and the compound **4** (0.70 g, yield 85%) was used directly in the next step.

Compound 1

Compound **4** (0.1 g, 0.34 mmol) and 2-hydroxy-1-napthaldehyde (0.07 g, 0.41 mmol) were dissolved in 5 mL of dry benzene and the reaction mixture was refluxed for 12 h. Then the solvent was removed under reduced pressure and the crude mass was thoroughly washed with diethyl ether to afford pure yellow coloured compound **1** in an excellent yield (0.097 g, 77%), mp 166 °C. ^{1}H NMR ($CDCl_3$, 400 MHz): δ 14.68 (brs, 1H), 8.93 (s, 1H), 7.94 (d, 1H, *J* = 8 Hz), 7.74 (d, 1H, *J* = 8 Hz), 7.68 (d, 1H, *J* = 8 Hz), 7.46 (t, 1H, *J* = 8 Hz), 7.28 (t, 1H, *J* = 8 Hz), 7.03 (d, 1H, *J* = 8 Hz), 5.38 (d, 1H, *J* = 4 Hz), 4.78–4.70 (m, 1H), 4.39 (s, 2H), 2.39–0.67 (m, 43H); ^{13}C NMR ($CDCl_3$, 100 MHz): 171.5, 168.2, 161.2, 139.2, 136.5, 133.2, 129.2, 127.9, 126.8, 123.1, 123.0, 122.9, 118.4, 107.8, 75.6, 56.6, 56.1, 49.9, 42.3, 39.7, 39.5, 38.0, 36.9, 36.5, 36.1, 35.8, 31.9, 31.8, 28.2, 28.0, 27.7, 24.2, 23.8, 22.8, 22.5, 21.0, 19.3, 18.7, 11.8; FTIR (KBr) *v* cm^{-1}: 3385, 2936, 1750, 1743, 1636, 1543, 1362. HRMS (TOF MS ES+): calcd. 598.4260 $(M + H)^+$, found 598.4290 $(M + H)^+$.

Gelation test

The relevant amount of compound **1** was dissolved in desired solvent (1 mL) forming a homogeneous solution, slightly warmed and then allowed to cool slowly to room temperature to form gel. Gel was tested by an inversion of vial method.

Determination of gel–sol transition temperature (T_g)

The gel-to-sol transition temperature (T_g) was measured by the dropping ball method. The T_g was defined as the temperature at which the gel was melted and started to flow. In this test, a small glass ball was carefully placed on the top of the gel to be tested, which was present in a test tube. The tube was slowly heated in a thermostated oil bath until the ball fell to the bottom of the test tube. The temperature at which the ball reaches the bottom of the test tube is taken as T_g of that system.

General procedure for fluorescence and UV–vis titrations

Stock solution of the compound **1** was prepared in desired solvent in the concentration range of 10^{-5} M. Stock solutions of anions were also prepared in the same solvent in the concentration range of 10^{-3} M. Solution of **1** (2 mL) was taken in the cuvette and to this solution different anions were individually added in different amounts. Upon addition of anions, the change in emission of the compound was recorded. The same stock solutions were used to perform the UV–vis titration experiment in the same way.

Supplementary material

Gelation results, emission, absorption, FTIR and ^{1}H NMR spectra, binding curves and copies of ^{1}H, ^{13}C NMR and HRMS.

Acknowledgments

We thank DST, West Bengal (Project No. 755(Sanc.)/ST/P/S&T/4G-3/2014, dated 27.11.2014) for providing financial assistance. SP thanks CSIR, New Delhi, India for a fellowship.

Disclosure statement

No potential conflict of interest was reported by the authors.

References

(1) *Ullman's Encyclopedia of Industrial Chemistry*, 6th ed.; Wiley-VCH: New York, 1998.
(2) Kirk, K.L. *Biochemistry of the Elemental Halogens and Inorganic Halides*; Plenum: New York, 1991; p 591.
(3) Sessler, J.L.; Gale, P.A.; Cho, W.S. *Anion Receptor Chemistry*; The Royel Society of Chemistry: Cambridge, 2006.
(4) Mathews, C.P.; van Hold, K.E. *Biochemistry*; Benjamin/Cummings: Redwood City, CA, 1990.
(5) Zweep, N.; van Esch, J.H. *Functional Molecular Gels*; The Royal Society of Chemistry, 2014, 1–29.
(6) Li, A.F.; Wang, J.H.; Wang, F.; Jiang, Y.B. *Chem. Soc. Rev.* **2010**, *39*, 3729–3745.
(7) Martínez-Máñez, R.; Sancenón, F. *Chem. Rev.* **2003**, *103*, 4419–4476.
(8) Nishiyabu, R.; Kubo, Y.; James, T.D.; Fossey, J.S. *Chem. Commun.* **2011**, *47*, 1106–1123.
(9) Amendola, V. *Chem. Soc. Rev.* **2010**, *39*, 3889–3915.
(10) Baird, C.; Cann, M. *Environmental Chemistry*; Freeman: New York, 2005.
(11) Vennesland, B.; Comm, E.E.; Knownles, C.J.; Westly, J.; Wissing, F. *Cyanide in Biology*; Academic Press: London, 1981.
(12) Koenig, R. *Science* **2000**, *287*, 1737–1738.
(13) Xu, Z.; Chen, X.; Kim, H.N.; Yoon, J. *Chem. Soc. Rev.* **2010**, *39*, 127–137.
(14) Kim, Y.; Zhao, H.; Gabbaï, F.P. *Angew. Chem. Int. Ed.* **2009**, *48*, 4957–4960.
(15) Wu, J.; Liu, W.; Ge, J.; Zhang, H. *Chem. Soc. Rev.* **2011**, *40*, 3483–3495.
(16) Ma, J.; Dasgupta, P.K. *Anal. Chim. Acta* **2010**, *673*, 117–125.
(17) Cheng, X.; Tang, R.; Jia, H.; Feng, J.; Qin, J.; Li, Z. *ACS Appl. Mater. Interfaces* **2012**, *4*, 438–446.
(18) Na, Y.J.; Park, G.J.; Jo, H.Y.; Lee, S.A.; Kim, C. *New J. Chem.* **2014**, *38*, 5769–5776.
(19) Divya, K.P.; Sreejith, S.; Balakrishna, B.; Jayamurthy, P.; Anees, P.; Ajayaghosh, A. *Chem. Commun.* **2010**, *46*, 6069–6071.
(20) Randviir, E.P.; Banks, C.E. *Trend. Anal. Chem.* **2015**, *64*, 75–85.
(21) Mohr, G.J. *Anal. Bioanal. Chem.* **2006**, *386*, 1201–1214.
(22) Pati, P.B. *Sens. Actuat. B* **2016**, *222*, 374–390.
(23) Sun, J.; Liu, Y.; Jin, L.; Chen, T.; Yin, B. *Chem. Commun.* **2016**, *52*, 768–771.
(24) Lin, Q.; Lu, T.T.; Zhu, X.; Sun, B.; Yang, Q.P.; Wei, T.B.; Zhang, Y.M. *Chem. Commun.* **2015**, *51*, 1635–1638.
(25) Lin, Q.; Sun , B.; Yang , Q.P.; Fu, Y.P.; Zhu, X.; Wei, T.B.; Zhang, Y.M. *Chem. Eur. J.* **2014**, *20*, 11457–11462.
(26) Kartha, K.K.; Babu, S.S.; Srinivasan, S.; Ajayaghosh, A. *J. Am. Chem. Soc.* **2012**, *134*, 4834–4841.
(27) Babu, S.S.; Praveen, V.K.; Ajayaghosh, A. *Chem. Rev.* **2014**, *114*, 1973–2129.
(28) Kartha, K.K.; Sandeep, A.; Praveen, V.K.; Ajayaghosh, A. *Chem. Rec.* **2015**, *15*, 252–265.
(29) Ghosh, K.; Kar, D.; Panja, S.; Bhattacharya, S. *RSC Adv.* **2014**, *4*, 3798–3803.
(30) Ghosh, K.; Panja, S.; Bhattacharya, S. *RSC Adv.* **2015**, *5*, 72772–72779.
(31) Ghosh, K.; Panja, S. *RSC. Adv.* **2015**, *5*, 12094–12099.
(32) Ghosh, K.; Kar, D. *Org. Biomol. Chem.* **2012**, *10*, 8800–8807.
(33) Ghosh, K.; Kar, D.; Bhattacharya, S. *Supramol. Chem.* **2014**, *26*, 313–320.
(34) Datta, S.; Bhattacharya, S. *Chem. Commun.* **2012**, *48*, 877–879.
(35) Dubey, M.; Kumar, A.; Gupta, R.K.; Pandey, D.S. *Chem. Commun.* **2014**, *50*, 8144–8147.
(36) Fan, K.; Song, J.; Li, J.; Guan, X.; Tao, N.; Tong, C.; Shen, H.; Niu, L. *J. Mater. Chem. C* **2013**, *1*, 7479–7482.
(37) Wang, C.; Chen, Q.; Sun, F.; Zhang, D.; Zhang, G.; Huang, Y.; Zhao, R.; Zhu, D. *J. Am. Chem. Soc.* **2010**, *132*, 3092–3096.
(38) Svobodová, H.; Noponen, V.; Kolehmainen, E.; Sievänen, E. *RSC Adv.* **2012**, *2*, 4985–5007.
(39) Würthner, F.; Kaiser, T.E.; Saha-Möller, C.R. *Angew. Chem. Int. Ed.* **2011**, *50*, 3376–3416.
(40) Hong, Y.; Lam, J.W.Y.; Tang, B.Z. *Chem. Soc. Rev.* **2011**, *40*, 5361–5388.
(41) Kobayashi, T. J-Aggregates; World Scientific: Singapore, 1996, Vol. 2.
(42) Rasale, D.B.; Maity, I.; Das, A.K. *Chem. Commun.* **2014**, *50*, 11397–11400.

(43) Basak, S.; Nanda, J.; Banerjee, A. *Chem. Commun.* **2013**, *49*, 6891–6893.
(44) Hong, Y.; Lam, J.W.Y.; Tang, B.Z. *Chem. Soc. Rev.* **2011**, *40*, 5361–5388.
(45) Wei, T.-B.; Li, W.-T.; Li, Q.; Su, J.-X.; Qu, W.-J.; Lin, Q.; Yao, H.; Zhang, Y.-M. *Tetrahedron Lett.* **2016**, *57*, 2767–2771.
(46) Wei, T.B.; Yan, G.T.; Li, H.; Zhu, Y.R.; Shi, B.B.; Lin, Q.; Yao, H.; Zhang, Y.M. *Supramol. Chem.* **2016**, *28*, 720–726. doi: 10.1080/10610278.2015.1125899.
(47) Padalkar, V.S.; Seki, S. *Chem. Soc. Rev.* **2016**, *45*, 169–202.
(48) Demchenko, A.P.; Tang, K.C.; Chou, P.T. *Chem. Soc. Rev.* **2013**, *42*, 1379–1408.
(49) Chou, P.T.; Wu, G.R.; Wei, C.Y.; Cheng, C.C.; Chang, C.P.; Hung, F.T. *J. Phys. Chem B* **2000**, *104*, 7818–7829.
(50) Sarkar, A.R.; Heo, C.H.; Park, M.Y.; Lee, H.W.; Kim, H.M. *Chem. Commun.* **2014**, *50*, 1309–1312.